

Vanadium-Containing Polyphosphomolybdate Immobilized on TiO₂ Nanoparticles: A Recoverable and Efficient Catalyst for Photochemical, Sonochemical and Photosonochemical Degradation of Dyes under Irradiation of UV Light

S. Tangestaninejad^{a*}, M. Moghadam^{a,b}, V. Mirkhani^a, I. Mohammadpoor-Baltork^a and H. Salavati^c

^aDepartment of Chemistry, University of Isfahan, Isfahan, 81746-7344, Iran

^bDepartment of Nanotechnology Engineering, University of Isfahan, Isfahan 81746-73441, Iran

^cDepartment of Chemistry, Payame Noor University (PNU), 81395-671, Isfahan, Iran

(Received 22 May 2009, Accepted 4 April 2010)

A new photocatalyst, nanoporous anatase TiO₂ crystalline particles coupled by Na₃PV₂Mo₁₀O₄₀ Keggin units, TiO₂-PVMo, was prepared by combination of the methods of sol-gel and hydrothermal treatment. The catalyst was characterized by X-ray diffraction (XRD), UV diffuse reflectance spectroscopy (UV-DRS), FT-IR spectroscopy, Scanning Electron Microscopy (SEM) and cyclovoltametry (CV). This photocatalyst exhibited a good photocatalytic (UV region) and sonocatalytic activity in the decomposition of different dyes in aqueous systems. The TiO₂-PVMo composite showed higher photocatalytic and sonocatalytic activity than pure polyoxometalate or pure TiO₂.

Keywords: Polyoxometalate, Photocatalytic, Sonocatalytic, Degradation, Dyes

INTRODUCTION

Polyoxometalates are excellent acid and oxidation catalysts as well as effective photocatalysts, whose photochemical activities originate from their unique structures [1-6]. POMs anions were good multielectron acceptors, and some saturated Keggin-type clusters such as PW₁₂O₄₀³⁻ and SiW₁₂O₄₀⁴⁻ showed satisfactory photoactivities in homogenous phase systems [7]. Among the photocatalysts, TiO₂ (in anatase phase) has been most widely used because it is easily available, inexpensive, non-toxic, photostable, its unique photochemical properties and shows relative high chemical stability [8, 9].

Although POMs exhibit UV-light photocatalytic activity in homogenous system, the main disadvantages of them as

photocatalysts lie in their low surface area and difficulty of separation from the reaction mixture. Therefore, development of novel solid catalysts with advanced characteristics such as surface area and porosity has been a challenge for a long time. Recent studies showed that immobilization of soluble POM units into the suitable supports (i.e. silica mesoporous molecular sieve MCM-41 or MCM-48, NaY zeolite, activated carbons, layered double hydroxide, amorphous or anatase TiO₂) are effective methods to overcome the mentioned problems [10-12].

In order to improve the photocatalytic activity of either POM or TiO₂ and heterogenization of soluble POM, POM can be supported on TiO₂. The motivation for this design is based on the structural characteristics of either TiO₂ or POM. That is, POM has empty d orbitals and can be used as good electron acceptors. After the addition of POM into TiO₂ photocatalytic

*Corresponding author. E-mail: stanges@sci.ui.ac.ir

systems, the fast charge-pair (h^+e^-) recombination on TiO_2 can be retarded effectively.

On the other hand, POM has the ability to enhance the rate of conduction band (CB) electron transfer by accepting e^- (photogenerated electrons) to its empty d orbitals. Several research groups have studied this synergistic effect between TiO_2 and POM [13-15].

Recent investigations have showed that reactive dyes can be decolorized by advanced oxidation process [18] involving the generation of powerful oxidizing agent like hydroxyl radicals ($\cdot OH$), which completely destroy the pollutants in wastewater. The hydroxyl radicals are capable of mineralizing all organic compounds almost to carbon dioxide (CO_2) and water (H_2O) as well as other simple inorganic ions. Heterogenous photocatalysis through illumination of UV [19] or solar light [20] on a semiconductor surface is an attractive advanced oxidation process. The chemical effect of high intensity ultrasound result primarily from acoustic cavitation: the formation, growth, and impulsive collapse of bubbles in liquids. In sonophotocatalysis, due to the generation of sites of high temperature and pressure by acoustic cavitation, overall water splitting was proposed to proceed by a two-step reaction as reported in literature [21]. The simultaneous use of two techniques was reported to be more effective than their sequential combination though leading to just additive effects, and to be more effective than sonolysis only when employing relative low ultrasound intensity [22]. Moreover, the ultrasound can usually be competent for catalyzing those chemical reactions that the ultraviolet and visible lights catalyze [23]. Synergistic effects have been evidenced by comparing kinetic results obtained by photocatalytic and sonophotocatalytic treatment [24].

Ultrasound affects the rate of the photocatalytic degradation of organic dyes and a synergistic effect between sonolysis and photocatalysis was observed, which may result from three different phenomena. First of all, ultrasound may induce the deaggregation of the photocatalyst, leading to an increase in its surface and thus in its catalytic performance. Then, it induces mass transport acceleration of chemical species between the solution phase and the photocatalyst surface and vice versa. Indeed, the observed desorption of organic species from the semiconductor surface might also have some role, even if not necessarily positive, in modifying

the degradation rate under photocatalysis. The main effect of ultrasound is to contribute through cavitation to scissor the H_2O_2 produced by both photocatalysis and sonolysis. This increases the amount of reactive radical species inducing oxidation of the substrate and of degradation intermediates and is the main responsible for the observed synergy.

The goal of this work is combining the TiO_2 and POMs by chemical interactions. This combination leads to preparation of more active catalysts which can be more easily handled for recycling and reuse [16, 17]. By consideration of TiO_2 and PVMo properties, nanoporous anatase TiO_2 particles coupled with homogenous PVMo were prepared at 200 °C via combination of the sol-gel technique with the programmed temperature hydrothermal method. The photocatalytic activity of the nanoporous TiO_2 -PVMo composite in the ultraviolet region was investigated in the degradation of different dyes.

EXPERIMENTAL

Materials and apparatus

All chemicals were used as received from different commercial sources (Merck, Aldrich and Fluka). Diffuse reflectance spectra, was recorded on a Shimadzu UV-265 instrument using optical grade $BaSO_4$ as the reference. FT-IR spectra were obtained as potassium bromide pellets in the range of 400-4000 cm^{-1} with Nicolet Impact 400D spectrometer. Scanning electron micrographs of the catalyst were taken on SEM Philips XL 30. XRD patterns were recorded on a D8 Advance Bruker, using $Cu K\alpha$ radiation ($2\theta=5-70^\circ$).

The $Na_5[PV_2Mo_{10}O_{40}] \cdot 14H_2O$ was prepared as described in the literature [25].

2.2. Preparation and characterization of TiO_2 -PVMo composite

The nanoporous TiO_2 -PVMo was prepared as following: Titanium tetraisopropoxide (TTIP, 98%, 6 mL) was dissolved with 30 mL of *iso*-propyl alcohol with stirring. A solution of $Na_5PV_2Mo_{10}O_{40}$ (0.4 g, 0.19 mmol) in water (0.8 mL), was added into the TTIP solution drop wise. The pH of resulting mixture was adjusted to 1-2 by addition of 8 M HCl, and was stirred at room temperature for 1 h. Then, the mixture was heated to 45 °C until homogenous TiO_2 -PVMo hydrogel was formed.

Vanadium-Containing Polyphosphomolybdate Immobilized on TiO₂ Nanoparticles

This hydrogel was heated in an autoclave in 200 °C with a heating rate of about 2 °C/min. Then hydrogel was cooled to room temperature and dehydrated slowly at 50 °C in vacuum for 24 h. The dried gel was washed with hot water and dried at room temperature (Scheme 1).

General procedure for photocatalytic degradation of dyes under irradiation of UV light

A photoreactor was designed with a cylindrical quartz cell configuration and an internal light source surrounded by a quartz jacket, where the suspension of the catalyst and aqueous dyes completely surrounded the light source. The temperature of the suspension was maintained at 20±1 °C by water circulation through an external cooling coil. The optical pathlength was ca. 2 cm. The light source was a 400 W high-pressure mercury lamp ($\lambda=200\text{-}380$ nm). The catalytic activity of the nanocomposite was tested using coperton Navy Blue-RL, Nylosan Black 2-BC, Methyl Orange, Congo Red, Solophenyl Red-3BL, Ponceau S, Bromothymol Blue, Methylene Blue and Rhodamin B as the targets.

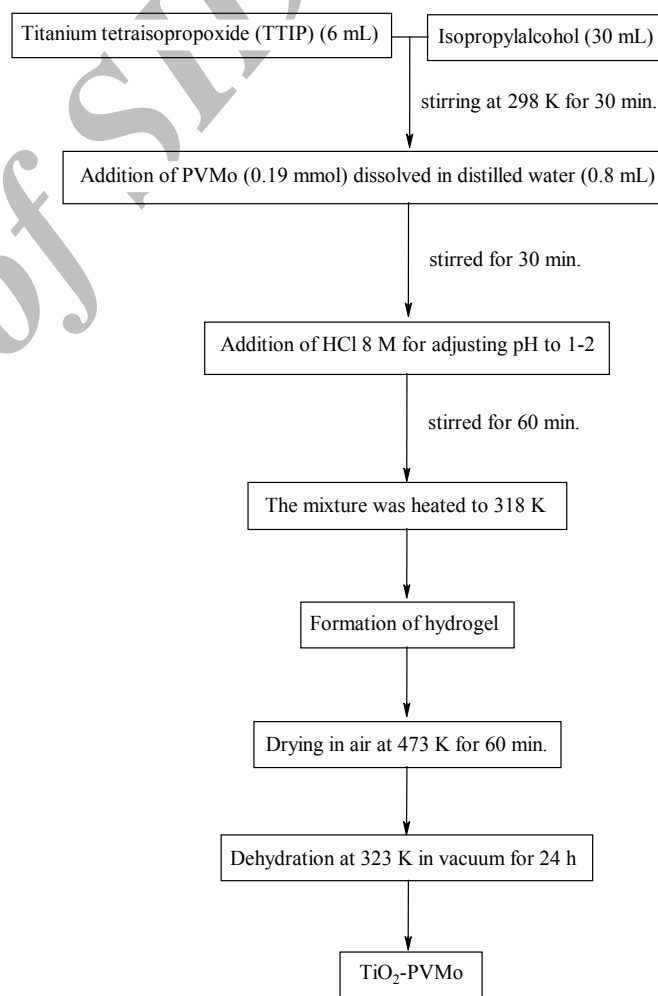
A general photocatalytic method was carried out as following: 50 mg of TiO₂-PVMo catalyst was suspended in 15 mL of fresh aqueous, dye solution (the dyes concentration is shown in Table 2). The suspension was stirred in the dark for 30 min to obtain a good dispersion and adsorption. The lamp was inserted around the suspension after its intensity became stable. Photodegradation of dye was carried out at atmospheric pressure using oxygen as oxidant in the batch photoreactor. After the reaction finished, the suspensions were centrifuged and filtered, the photolyte was analyzed by UV-Vis spectrophotometer at λ_{max} for each dye.

General procedure for degradation of dyes under ultrasonic irradiation

A UP 400S ultrasonic processor equipped with a 3 mm wide and 140 mm long probe, which was immersed directly into the reaction mixture, was used for sonication. The operating frequency was 24 kHz and the output power was 0-400 W through manual adjustment.

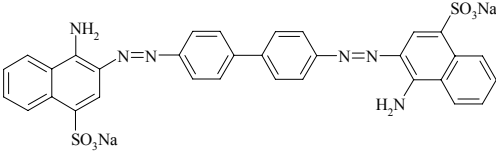
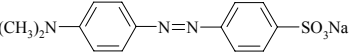
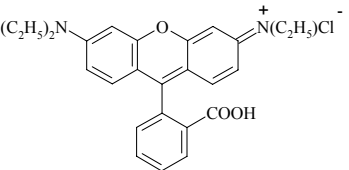
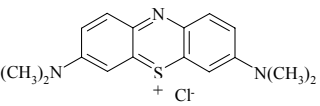
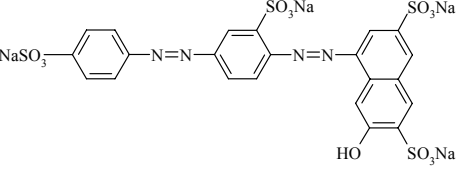
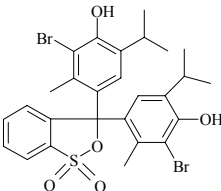
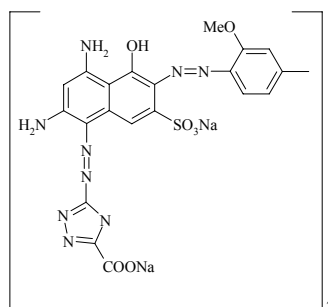
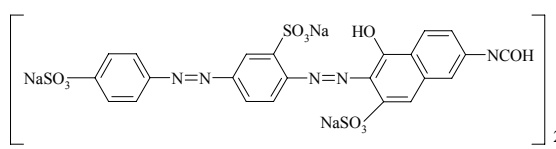
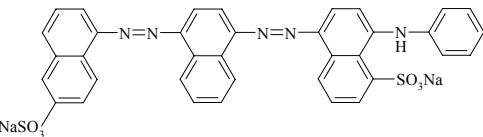
A 50 mg of TiO₂-PVMo catalyst was suspended in 15 mL of fresh aqueous, dye solution (the dyes concentration is shown in Table 2). The suspension was stirred in the dark for 30 min to obtain a good dispersion and adsorption. Then, the

solution was sonicated by ultrasonic waves. Photodegradation of dye was carried out at atmospheric pressure using oxygen as oxidant in the batch photoreactor. The temperature of the suspension was maintained at 20±1 °C by water circulation through an external cooling coil. After the reaction finished, the suspensions were centrifuged and filtered, the photolyte was analyzed by UV-Vis spectrophotometer at λ_{max} for each dye.



Scheme 1. Pathway of preparation of the TiO₂-PVMo composite

Table 1. Dyes structure used in this study

Dye	Chemical formula	MW (g/mol)
Congo Red (CR)		696.67
Methyl Orange (MO)		327.34
Rhodamine B (RB)		479.28
Methylene Blue (MB)		373.88
Ponceau S		760.56
Bromothymol Blue		624.40
Coperoxon Navy Blue RL		1110
Solophenyl Red-3BL		1373.3
Nylosan Black 2-BC		731.26

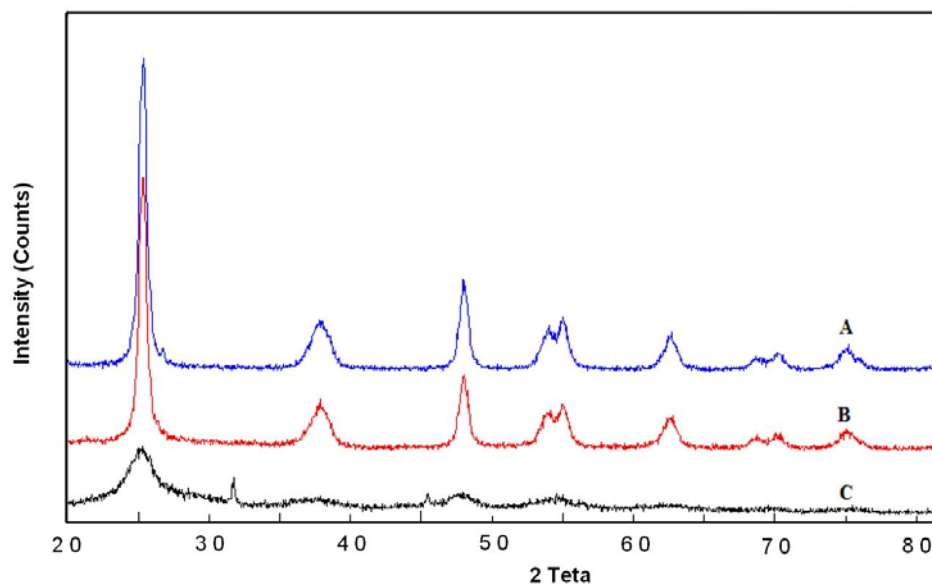


Fig. 1. XRD patterns of: (A) anatase TiO₂, (B) anatase TiO₂-PVMo composite, and (C) amorphous TiO₂-PVMo composite.

RESULTS AND DISCUSSION

Preparation and characterization of TiO₂-PVMo composite

Since heteropolyanions of the Keggin structure have molecular diameters of $\sim 12\text{\AA}$, it is feasible to support polyoxometalates such as PVMo into TiO₂. Fig. 1 shows the XRD patterns of TiO₂ and PVMo-TiO₂. These patterns showed the uniform anatase structure with its characteristic diffraction peaks of 2θ values at 25.4° , 37.8° , 48.0° , 54.5° , 62.7° , respectively [26]. However, PVMo-TiO₂ pattern (prepared via sol-gel procedure) indicated that PVMo was introduced either in the octahedral interstitial sites or the substitutional position of TiO₂ [27].

The XRD results were in accordance with the results obtained from the diffuse reflectance UV-Vis spectra. Diffuse reflectance (DR) UV-Vis spectra showed that the PVMo-TiO₂ crystallites exhibited broad and strong absorption in range of 200–400 nm, which was different from the original PVMo and anatase TiO₂ (Fig. 2). The results indicated that primary Keggin structure has been introduced into the nanostructure framework.

A red-shift (ca.15 nm) was observed compared with the anatase support. The red-shift and widening of this band have been attributed to a distorted tetrahedral coordination environment or the existence of some titanium species in an octahedral coordination environment [28]. Therefore, the introduction of polyoxometalate in TiO₂ framework results in the changes of coordination environment of TiO₂. Scanning electron micrographs (SEM) was recorded to obtain the shape and diameter of particles (Fig. 3). The results showed that spherical particles were well distributed and the average particle size was less than 80 nm.

Table 2. Optimization of catalyst amount in the degradation of MB.^a

Entry	Catalyst amount (mg)	Degradation yield (%)
1	10	20
2	20	52
3	30	63
4	40	78
5	50	94
6	60	94

^aReaction conditions: Catalyst; pH= 4.3; Oxygen flow rate= 5 mL/ min.

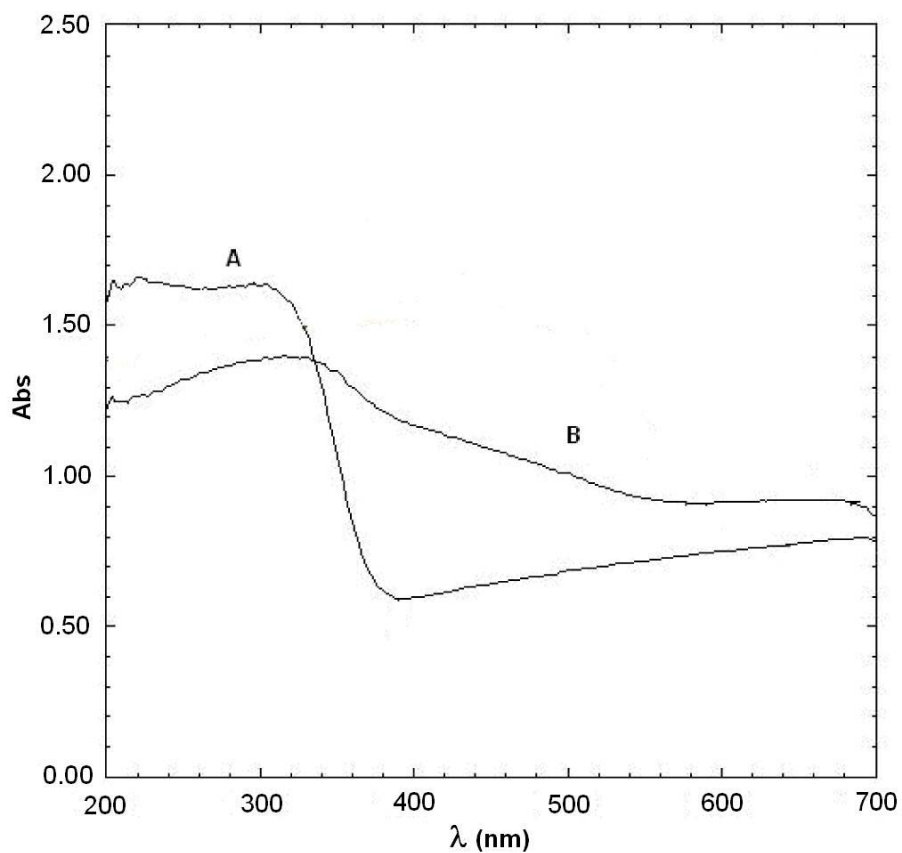


Fig. 2. DR UV-Vis spectra of: (A) anatase TiO_2 and (B) anatase TiO_2 -PVMO composite.

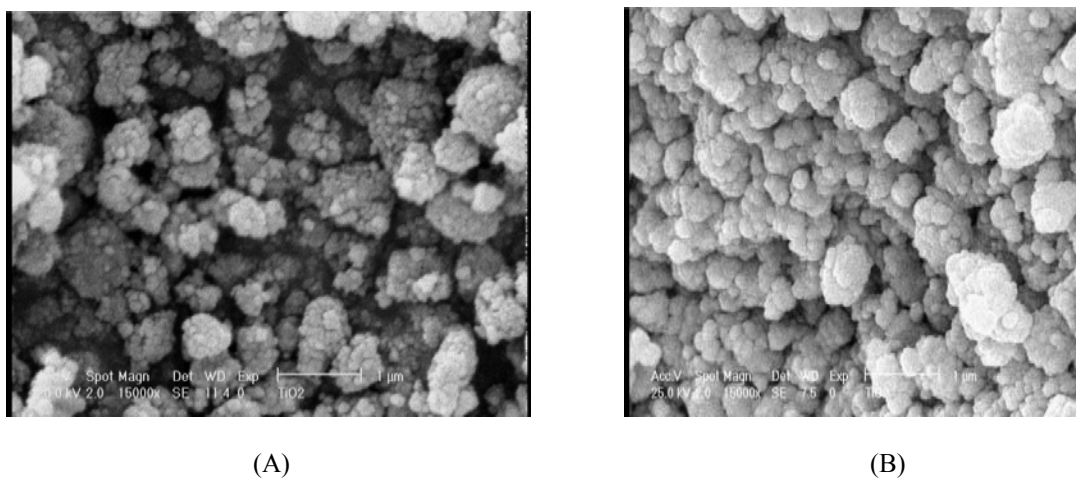


Fig. 3. SEM images of: (A) anatase TiO_2 and (B) anatase TiO_2 -PVMO composite

Vanadium-Containing Polyphosphomolybdate Immobilized on TiO₂ Nanoparticles

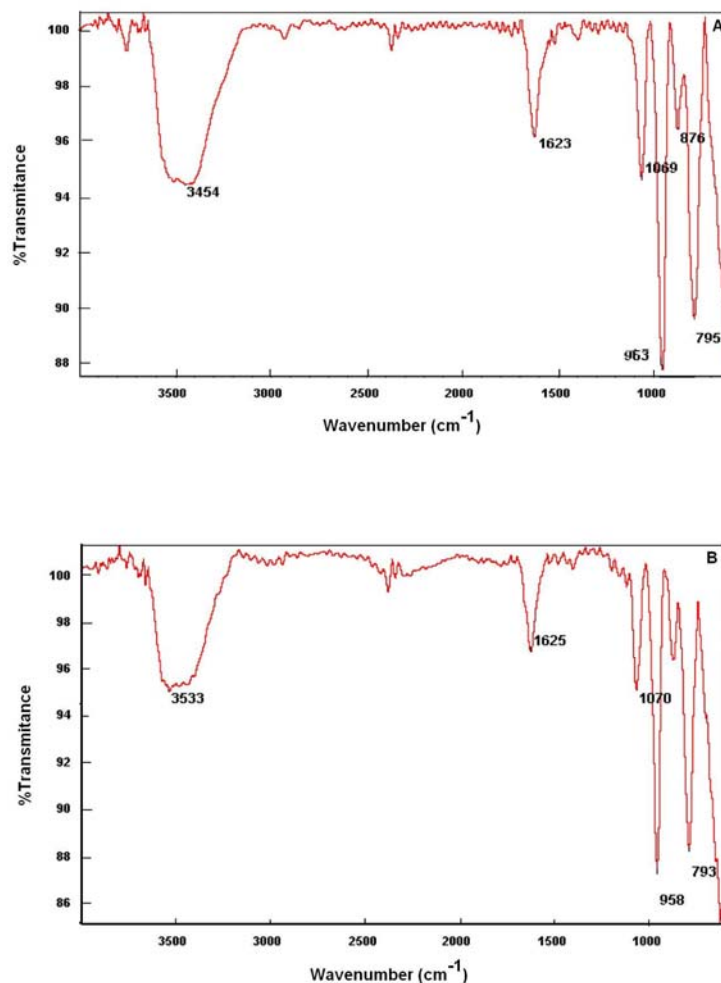


Fig. 4. FT-IR spectrum of: (A) anatase TiO₂-PVMO and (B) recovered TiO₂-PVMO

FT-IR Spectrum of the prepared catalyst in the range of 700-1100 cm⁻¹ showed absorption bands at 1072, 954, 869 and 793 cm⁻¹, corresponding to the four typical skeletal vibrations of the Keggin polyoxoanions, which indicated that PVMO has been supported on TiO₂ (Fig. 4). These bands could be attributed to ν(P-O), ν(Mo-O), ν(Mo-O_b-Mo), ν(Mo-O_c-Mo) (O_b: corner-sharing oxygen, O_c: edge-sharing oxygen), respectively [29]. In order to be able to investigate the electrochemical behavior of the PVMO supported on TiO₂, which is insoluble in water, three dimensional bulk modified carbon paste electrode (CPEs) employing PVMO supported on TiO₂ was fabricated by direct mixing. In this configuration, the

graphite powder contributes to the conductivity; silicon oil is as a pasting liquid; and supported PVMO act as the electroactive species. The electrochemical studies were carried out in 0.2 M H₂SO₄ aqueous solution, because PVMO is unstable in neutral and basic aqueous solutions. Figure 5 shows the cyclic voltammograms in 0.2 M H₂SO₄ aqueous solution at a bare CPE (curve a), and CPE modified with PVMO-TiO₂ (curve b). It can be seen from Figure 5 that in the potential range -0.30 to 1.4 V (vs. Ag/AgCl), there is no redox peak at the bare CPE, while at the modified CPE, some consecutive redox processes are observed. The above experimental results showed that PVMO can be supported on the surface of TiO₂.

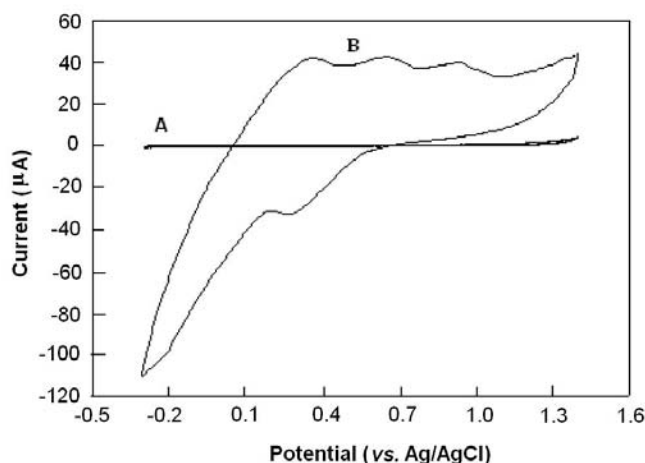


Fig. 5. Cyclic voltammograms of: (a) bare CPE; and (b) TiO₂-PVMO-CPE in 0.2 M H₂SO₄ solution. Scan rate: 100 mV s⁻¹.

Photocatalytic degradation of dyes

The structure of dyes and their λ_{max} are presented in Tables 1. First, the degradation of Methylene blue, MB, was investigated in aqueous solution under UV light irradiation. Since, the preadsorption of dyes before irradiation is very important for photocatalysis experiments, the preadsorption degree of MB by TiO₂-PVMO was measured at ca. 663 nm. The results showed that about 5% of MB molecules were absorbed on TiO₂-PVMO nanoparticles after 12 h.

In the photocatalytic experiments, the amount of catalyst, oxygen flow rate and pH were optimized in the degradation of MB under UV light. The disappearance of peak at $\lambda_{\text{max}} = 663$ nm was chosen for monitoring of the dye degradation (Fig. 6).

Table 3. Optimization of pH in the degradation of MB.^a

Entry	pH	Degradation yield (%)
1	2	50
2	3	68
3	4	87
4	4.3	95
5	5.8	78
6	9	74

^aReaction conditions: Catalyst (50 mg); Oxygen flow rate= 5 mL/ min.

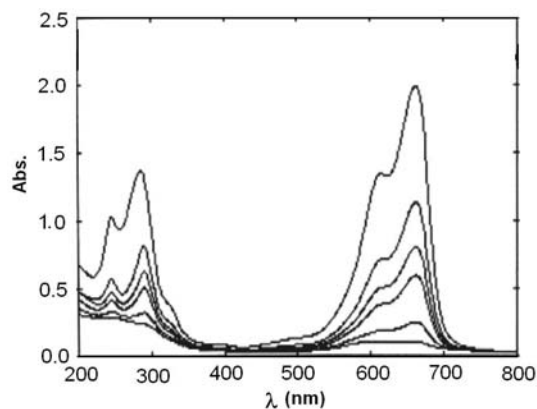


Fig. 6. Spectral change that occur during photocatalytic degradation of aqueous solution of MB: pH= 4.3; Catalyst (50 mg); C₀= 10 ppm; Oxygen flow rate= 5 mL/ min.

The results showed that the degradation percent was 94% in the presence of 50 mg of catalyst and irradiation of UV light for 30 min at room temperature (Table 2). Experiments showed that the presence of oxygen is necessary for degradation process. In the absence of oxygen, the degradation percent was 25%. While, in a flow of 5 mL/min of oxygen gas, the highest degradation yield was obtained (Table 3). The effect of pH of solution was also investigated on the degradation rate of MB. The obtained results showed that the degradation ratio was higher at pH= 4.3 (Fig. 7 and Table 4). These optimized conditions were used for degradation of different dyes. As shown in Table 5, the TiO₂-PVMO is an efficient photocatalyst for degradation of organic dye pollutants such as Coperoxon Navy (Co) Blue-RL, Nyson

Table 4. Optimization of oxygen flow rate in the degradation of MB.^a

Entry	Oxygen flow rate (mL/min)	Degradation yield (%)
1	0	25
2	2	51
3	3	73
4	5	94
5	7	86
6	10	61

^aReaction conditions: Catalyst (50 mg); pH= 4.3.

Vanadium-Containing Polyphosphomolybdate Immobilized on TiO₂ Nanoparticles

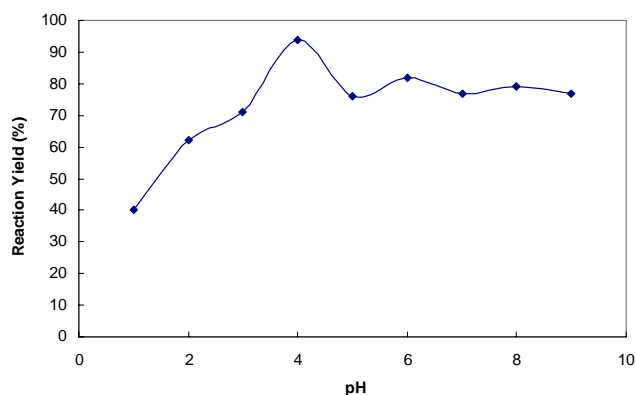


Fig. 7. Effect of pH on the photocatalytic degradation of aqueous solution of MB: Catalyst (50 mg); $C_0 = 10$ ppm; Oxygen flow rate = 5 mL/min.

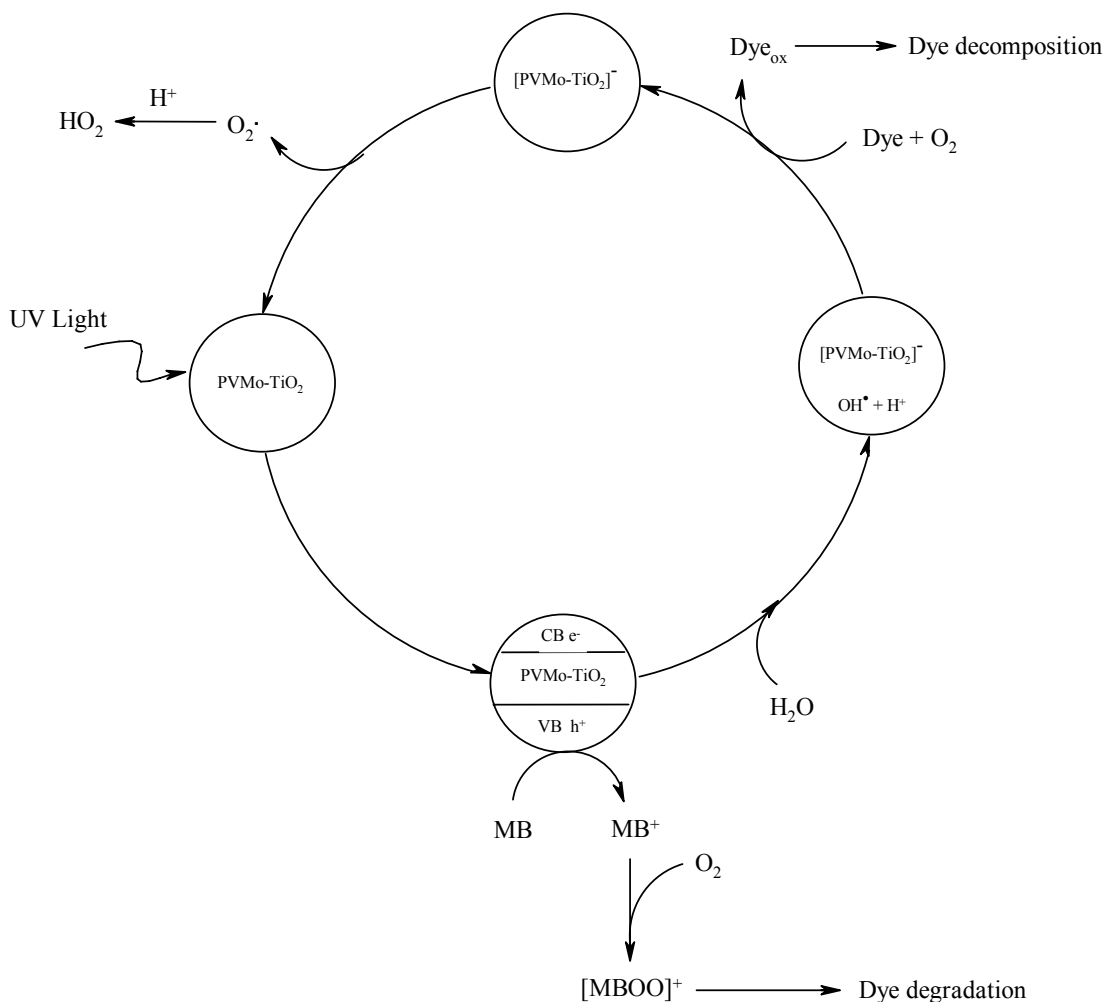
Black 2-BC (Ny), Methyl Orange (MO), Congo Red (CR), Solophenyl Red-3BL (SR), Ponceau S (PS), Bromothymol Blue (BT), and Rhodamin B (RB) under irradiation of UV light. In order to show the effect of PVMo in the photocatalytic activity of TiO₂, all reactions were repeated

under the same reaction conditions using TiO₂ as photocatalyst. The results showed that the photocatalytic activity of TiO₂ has increased by introducing of PVMo. However, a plausible pathway for degradation of dyes is shown in Scheme 2 [30]. In the direct photocatalysis, both positive holes and hydroxyl radicals have been proposed as the oxidizing species responsible for initiating the degradation of the organic substrates. Two possible mechanisms have been proposed. The first mechanism is that when photocatalytic oxidation is conducted in the presence of water, the holes were efficiently scavenged by water and generated hydroxyl radicals OH[•], which are strong and unselected oxidant species in favor of totally oxidative degradation and mineralization for organic substrates. The second one is that substrates (dyes) with the proper oxidation potential can undergo direct oxidation, and generate radical species. In the photocatalysis, the PVMo/TiO₂ nanocomposite absorbed UV-light to produce electron/hole (e./h+) pairs. Some organic dyes can be strongly absorbed on the PVMo/TiO₂ surface (Scheme 2). For example, MB is mainly oxidized by photogenerated hole localized on the surface of the irradiated catalyst, generated an adsorbed MB cation radical (MB^{•+})[30].

Table 5. Photocatalytic, sonocatalytic and sonophotocatalytic degradation of dyes catalyzed by TiO₂-PVMo^a under irradiation of UV light.

Entry	Dye	TiO ₂			TiO ₂ -PVMo			TiO ₂ -PVMo			TiO ₂ -PVMo			Conc. (ppm)	λ_{max}
		(Photocatalytic)			(Photocatalytic)			(Sonocatalytic)			(Photo-sonocatalytic)				
		Yield (%)	Time (min)	k (min ⁻¹)	Yield (%)	Time (min)	k (min ⁻¹)	Yield (%)	Time (min)	k (min ⁻¹)	Yield (%)	Time (min)	k (min ⁻¹)		
1	Coperoxon Navy Blue -RL	55	20	0.021	88	20	0.082	82	20	0.075	97	20	0.12	60	570
2	Nylosan black 2-BL-Acid black	69	15	0.022	93	15	0.117	86	15	0.095	100	15	0.15	200	568
3	Methyl Orange	58	20	0.026	90	20	0.095	75	20	0.092	98	20	0.135	20	462
4	Congo Red	47	20	0.026	87	20	0.092	78	20	0.087	97	20	0.13	40	498
5	Solophenyl Red-3BL	60	20	0.035	92	20	0.089	84	20	0.079	99	20	0.124	40	530
6	Ponceau S	62	20	0.032	91	20	0.13	83	20	0.11	98	20	0.185	30	520
7	Bromothymol Blue	49	30	0.031	89	30	0.18	79	30	0.17	98	30	0.24	40	435
8	Methylene Blue	70	15	0.052	94	15	0.35	85	15	0.32	100	15	0.48	10	663
9	Rhodamin B	59	25	0.043	86	25	0.18	80	25	0.19	98	25	0.28	30	557

^aReaction conditions: Catalyst (50 mg); pH = 4.3; Oxygen flow rate = 5 mL/min.



Scheme 2. Proposed mechanism for photodegradation of dyes in the presence of PVMo / TiO_2

Pure anatase TiO_2 has no synergistic effect, therefore the interfacial electron transfer takes place in TiO_2 itself, resulting in the fast electron-hole recombination. Therefore, the photocatalytic efficiency of anatase TiO_2 under UV irradiation was lower.

In addition of lower degradation yield in the case of anatase TiO_2 , another disadvantage of it, is its separation from aqueous solution. In this case, a milky solution is produced in which TiO_2 cannot be easily separated from solution even after several hours centrifugation. This may be due to the presence of fine TiO_2 particles and its low bulk density. Therefore, the TiO_2 -PVMo can be reused more easily than pure TiO_2 .

The higher photocatalytic activity of TiO_2 -PVMo in comparison with anatase TiO_2 photocatalyst and PVMo in the degradation of dyes mainly originated from the synergistic effect due to combination of PVMo and TiO_2 . The synergistic effect is that in the system of anatase TiO_2 nanoparticles coupled by Keggin PVMo units, the interfacial electron transfer takes place from the TiO_2 conduction band to PVMo by light irradiation. Such an effective electron transfer can inhibit the fast electron-hole recombination on TiO_2 , and the trapped holes have sufficient time to react with H_2O to generate OH radicals. The OH radicals photooxidize the MB, and then decolorized the solution.

Pure anatase TiO₂ has no the synergistic effect, therefore the interfacial electron transfer takes place in TiO₂ itself, resulting in the fast electron-hole recombination. Therefore, the photocatalytic efficiency of anatase TiO₂ under UV irradiation was lower [15,30].

In order to show the commercial applicability of this method in the degradation of dyes, a sample of MB was placed under irradiation of solar light. The results showed that after 60 min the MB was completely degraded.

Sonocatalytic degradation of dyes

Another interesting alternative for the degradation of pollutants in the waste water is sonocatalysis, which can be used instead of photocatalysis [31, 32]. Therefore, the effect of ultrasonic irradiation on the dyes degradation by TiO₂-PVMo was also investigated. First, the sonodegradation of MB was investigated under the same reaction conditions described for degradation under UV light (15 mL of 10 ppm MB, 50 mg catalyst, pH= 4.3, and oxygen flow rate= 5 mL/ min). Irradiation with the ultrasonic waves for 15 min caused a significant decrease in the absorption at 663 nm, which indicated that more than 84% of MB has been degraded under sonication. While, in the presence of TiO₂ under sonication, only 40% of MB was degraded. The ability of ultrasonic irradiation in the degradation of different dyes is shown in Table 5. The power of ultrasound is a very important parameter that has also a great influence on the phenomena of acoustic cavitation and efficiency of ultrasound treatment. Fig. 8 shows the effect of irradiation power on the degradation of MB, which indicates that increasing of ultrasound power will improve the extent of degradation and the higher conversion, was observed at 400 W. Sonocatalytic degradation of dyes in the presence of photocatalysts has been reported in several papers. It is mentioned that the oxidation process of dyes is [•]OH dependent [33]. Therefore, the presence of TiO₂-PVMo in an ultrasonic system should results in the formation of [•]OH in the irradiated solutions. Increasing in the formation of [•]OH can be explained by well-known mechanism of hot spots and sonoluminescence as follows. First, cavitation can be increased due to the heterogeneous nucleation of bubbles, resulting in the induction of hot spots in the solution. Very high temperatures can be reached in these hot spots and can

cause the pyrolysis of H₂O molecules to form [•]OH. The produced H₂O₂ by recombination of [•]OH may also interact with the surface of TiO₂ and produce a number of oxidizing agents, which can facilitate the dyes degradation. Second, sonoluminescence which causes by ultrasound involves an intense UV light and excite the TiO₂ particles to act as a photocatalyst during sonication.

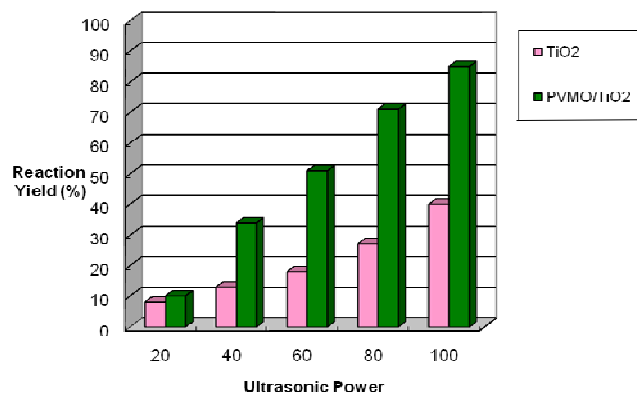


Fig. 8. The effect of ultrasonic irradiation power on the sonodegradation of MB: pH= 4.3; Catalyst (50 mg); C₀= 10 ppm; Oxygen flow rate= 5 mL/ min.

Sonophotocatalytic degradation of dyes

The simultaneous use of photocatalysis and sonocatalysis, sonophotocatalysis, is more effective than sequential combination. Such combination leads to additive effects and is effective than sonolysis and photolysis only. Therefore, sonophotocatalytic degradation of dyes was investigated under ultrasonic and UV light irradiation. All reactions were carried out under the same reaction conditions which are described for photolysis and sonolysis. The results, Table 5, showed that the sonophotocatalytic activity of TiO₂-PVMo was higher than those of the direct photolysis and sonolysis by TiO₂.

Catalyst reuse

After the reaction was finished, the suspension was centrifuged, and the TiO₂-PVMo catalyst was easily recovered by sedimentation, and the recovered catalyst was washed with water and ethanol, successively. The amount of Mo leached, in

Table 6. The results of TiO₂-PVMo catalyst reuse and Mo leached in the degradatin of MB by photolysis, sonolysis and sonophotolysis.

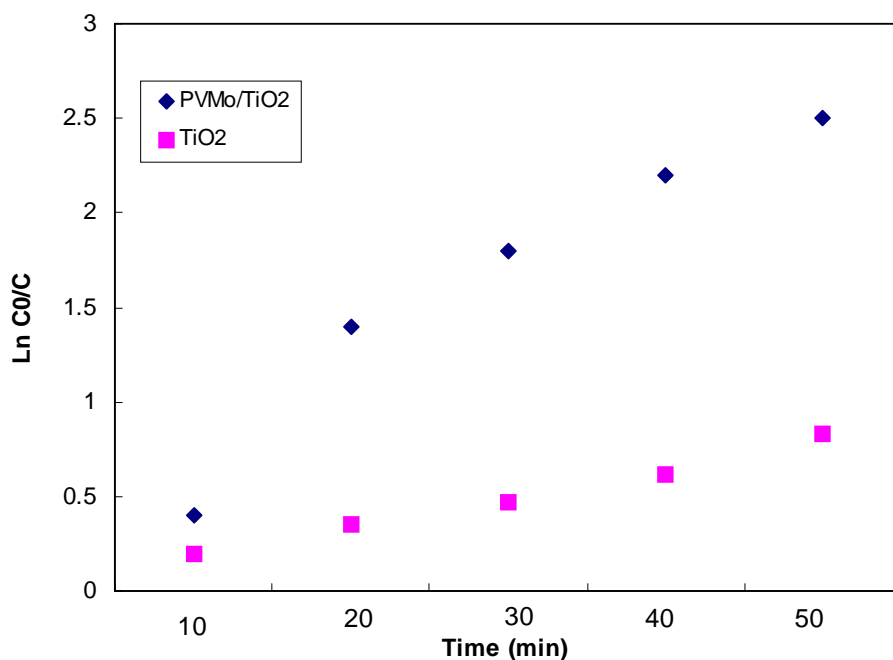
Run	TiO ₂ -PVMo (Photocatalytic)			TiO ₂ -PVMo (Sonocatalytic)			TiO ₂ -PVMo (Photo-sonocatalytic)		
	Yield (%)	Time (min)	Mo leached (%)	Yield (%)	Time (min)	Mo leached (%)	Yield (%)	Time (min)	Mo leached (%)
1	94	15	1.7	85	15	2	100	15	2
2	92	15	1	83	15	1.5	97	15	1.5
3	91	15	0	80	15	0.5	96	15	1
4	90	15	0	80	15	0	95	15	0

the clear solution, was determined by ICP. The results showed that about 2% of Mo has been leached from catalyst. These results are attributed to strong coordination interactions between the Keggin unit and the titania surface. More importantly, the interaction between the Keggin unit and TiO₂ support is chemical rather than physical. Therefore, the composite could be reused four times without significant loss of its photocatalytic activity. The results are summarized in Table 6.

Photocatalytic kinetics

MB was chosen as a model substrate for investigation of dyes degradation kinetics in aqueous solution under UV, ultrasonic and combination of UV and ultrasonic irradiation. The results are shown on Fig. 9. It follows an apparent first-order in agreement with a generally observed Langmuir-Hinshelwood kinetics model:

$$r = \frac{dC}{dt} = \frac{kKC}{1+KC}$$

**Fig. 9.** First-order linear $\ln (C_0/C) = f(t)$ for TiO₂-PVMo and TiO₂

Where r is the degradation rate of the reactant (mg/l min), C is the concentration of the reactant (mg/l), t is the irradiation time, k is the reaction rate constant (mg/l min), and K is the adsorption coefficient of the reactant (l/mg). When the initial concentration C_0 is micromolar, the above equation can be simplified to an apparent first-order equation:

$$\ln(C_0/C) = k_{app}t$$

A plot of $\ln(C_0/C)$ versus time represents a straight line, the slope of which upon linear regression equals the apparent first-order rate constant k_{app} . The determined k_{app} values are summarized in Table 5.

CONCLUSION

This system introduces a simple and green heterogeneous photocatalytic approach for the degradation of organic dyes which are present in the textile industry.

The prepared composite was successfully used for photocatalytic, sonocatalytic and sonophotocatalytic degradation of different dyes in aqueous media. The high catalytic activity of TiO₂-PVMo is attributed to the synergistic effect between the PVMo and the anatase TiO₂. The TiO₂-PVMo catalyst can be easily separated and recovered, and deactivation of the catalysts was hardly observed after four catalytic recycling.

ACKNOWLEDGEMENTS

The financial support of this work by the Office of Strategies of New Technologies of Isfahan Province is acknowledged.

REFERENCES

- [1] T. Yamase, Chem. Rev., 98 (1998) 307.
- [2] R. C. Chambers, C. L. Hill, J. Am. Chem. Soc. 112 (1990) 8427.
- [3] T. Yamase, Inorg. Chim. Acta, 76 (1983) 125.
- [4] H. Einaga, M. Misono, Bull. Chem. Soc. Jpn. 70 (1997) 1551.
- [5] T. Okuhara, Chem. Rev., 102 (2002) 3641.
- [6] Y. Yang, Y. Guo, C. Hu, E. Wang, Appl. Catal. A: Gen. 252 (2003) 305.
- [7] D. Sattari, C.L. Hill, J. Am. Chem. Soc., 115 (1993) 4649.
- [8] D. Chatterjee, A. Mahata, Appl. Catal. B: Environ. 33 (2001) 119.
- [9] Y. Yang, Y. Guo, C. Hu, E. Wang, E. Wang, Appl. Catal. A: Gen. 273 (2004) 201.
- [10] R. R. Ozer, J. L. Ferry, J. Phys. Chem. B: Environ. 106 (2002) 4336.
- [11] M. Kang, Appl. Catal. B: Environ. 37 (2002) 187.
- [12] D. Li, Y. Guo, C. Hu, J. Mol. Catal. A: Chem. 207 (2004) 181.
- [13] X. Qu, Y. Guo, C. Hu, J. Mol. Catal. A: Chem. 262 (2007) 128.
- [14] R. O. Ruya, J. L. Ferry, J. Phys. Chem. B 106 (2002) 4336.
- [15] L. Li, Q. Wu, Y. Guo, C. Hu, Micropor. Mesopor. Mater. 87 (2005) 1.
- [16] Y. Guo, C. Hu, S. Jiang, C. Guo, Y. Yang, E. Wang, Appl. Catal. B: Environ. 36 (2002) 9.
- [17] Y. Yang, Y. Guo, C. Hu, C. Jiang, E. Wang, J. Mater. Chem. 13 (2003) 1686.
- [18] N. H. Ince, G. Tezcanli, R.K. Belen, I.G. Apikyan, Appl. Catal. B: Environ. 29 (2001) 167.
- [19] M. Saquib, M. Muneer, Dyes Pigm. 56 (2003) 37.
- [20] M. Muruganandham, M. Swaminathan, Sol. Energy Mater. Sol. Cells 81 (2004) 439.
- [21] H. Harada, C. Hosoki, A. Kudo, J. Photochem. Photobiol. A: Chem. 141 (2001) 219.
- [22] S. Kaur and V. Singh, Ultrason. Sonochem. 14 (2007) 531.
- [23] C. Petrier, K. Suslick, Ultrason. Sonochem. 7 (2000) 53.
- [24] M. Mrowetz, C. Pirola, E. Selli, Ultrason. Sonochem. 10 (2003) 247.
- [25] K. Nomiya, S. Matsuoka, T. Hasegawa, Y. Nemoto, J. Mol. Catal. A: Chem. 156 (2000) 143.
- [26] H. Zhu, J. A. Othman, J. Li, J. Zhuo, G. Churchman, E. Vansant, Chem. Mater. 14 (2002) 5037.

- [27] S. I. Shah, W. Li, C. P. Huang, G. Jung, C. Ni, PNAS 99 (2002) 6482.
- [28] T. Blasco, A. Corma, M. Navarro, J. Pariente, J. Catal. 156 (1995) 65.
- [29] Th. Ilkenhans, B. Herzag, Th. Braun, R. Schlogl, J. Catal. 153 (1995) 275.
- [30] Y. Yang, Q. Wu, Y. Guo, C. Hu, E. Wang, J. Mol. Catal A: Chem 225 (2005) 203.
- [31] J. Wang, B. Guo, X. Shang, Z. Shang, J. Han, J. Wu, Ultson. Sonochem. 12 (2005) 331.
- [32] K. Okitsu, K. Iwasaki, Y. Yobiko, H. Bandow, R. Nishimura, Y. Maeda, Ultson. Sonochem. 12 (2005) 255.

Archive of SID